

Linear and nonlinear dynamics in rotating flows

C. Cambon

Laboratoire de Mécanique des Fluides et d'Acoustique,
U.M.R n° 5509, Ecole Centrale de Lyon,
BP 163, 69131 Ecully Cedex, France

1 introduction

Structuring linear and nonlinear effects caused by Coriolis force, and/or buoyancy force in neutral and/or stably stratified fluid, are surveyed and discussed in this article.

Stability analysis is considered when the rotating flow consists of *preexisting* coherent large-scale vortices subject to three-dimensional disturbances. System rotation does not affect the motion of an incompressible two-dimensional (2D) flow but it alters its stability with respect to three-dimensional (3D) disturbances. When the background flow consists of arrays of vortices, this problem has many applications in geophysical or industrial flows. When considering both cyclonic and anticyclonic vortices in a rotating frame, it is well admitted that moderate anticyclones are preferentially destabilised, but explanations for this and precise ranges of parameters (Rossby number especially) are often not consistent in the literature. This problem, which has been the subject of an abundant literature, — with analyses, physical and numerical experiments —, is revisited in this paper by looking at the linear stability, *with system rotation*, of simple flows. Special emphasis will be placed on a street of Stuart vortices, an interesting model for the sheared mixing layer with spanwise billows. Results of classic analyses in terms of normal modes are briefly recalled and contrasted with results of an asymptotic analysis (Lifschitz & Hameiri, 1991) for short wave disturbances, which are localised around fluid trajectories.

A second line of attack, for dynamics of rotating turbulence, addresses the *creation* of structure through nonlinear interactions which are altered by Coriolis force. A similar approach is touched upon for stably stratified flows with and without rotation. This illustrates what can be explained from classical approaches to anisotropic homogeneous turbulence, taking advantage of close relationship between 'two-point closures theories' and 'weakly nonlinear theories for wave turbulence'. Anisotropic description allows to represent linear and nonlinear interactions in terms of detailed eigenmodes of motion, like 'vortex' and 'waves', including the angular dependence of related scalar spectra and cospectra in Fourier space. This anisotropic description was shown to be relevant to obtain precise indicators of the 'columnar' and 'pancake' structuring in physical space.

Additional effects of local forcing and confinement are investigated to understand the creation of coherent quasi-two dimensional vortices by pure rotation, from initially strongly three-dimensional, unstructured turbulence.

'Rapid Distortion Theory' (RDT hereinafter) for homogeneous turbulence plays a central role in both linear stability analysis and turbulence modelling. On the one hand,

the asymptotic method (Lifschitz & Hameiri, 1991) can be considered as a zonal ‘RDT’ approach to the linear stability of nonhomogeneous flows with coherent vortices. On the other hand, ‘homogeneous RDT’ provides crucial building blocks for nonlinear theories, such as the basis of eigenmodes and related dispersion relationships, in homogeneous, rotating and/or stably stratified turbulence, or wave-turbulence.

Background equations are recalled in the following, with the essentials for understanding internal waves regimes. Navier-Stokes equations with the Boussinesq approximation in a rotating frame are

$$(\partial_t + \mathbf{u} \cdot \nabla)\mathbf{u} + 2\Omega\mathbf{n} \times \mathbf{u} + \nabla p - \nu\nabla^2\mathbf{u} = \mathbf{n}b \quad (1)$$

$$(\partial_t + \mathbf{u} \cdot \nabla)b - \chi\nabla^2b = -N^2\mathbf{n} \cdot \mathbf{u} \quad (2)$$

$$\nabla \cdot \mathbf{u} = 0 \quad (3)$$

where \mathbf{u} , p and b are the fluctuating velocity, pressure (divided by mean density of reference), and buoyancy force intensity, respectively. \mathbf{n} denotes the vertical unit upward vector with which are aligned both the gravitational acceleration, $\mathbf{g} = -g\mathbf{n}$, and the angular velocity of the rotating frame $\boldsymbol{\Omega} = \Omega\mathbf{n}$. The buoyancy force is related to the fluctuating temperature field τ by $\mathbf{b} = -\mathbf{g}\beta\tau$, through the coefficient of thermal expansivity β , and the temperature stratification is characterized by the vertical gradient γ . Using b instead of τ in the first two equations above yields introducing the Brunt-Waisala frequency N only as the characteristic frequency of buoyancy-stratification, with $N = \sqrt{\beta g \gamma}$. Hence the linear operators in equations (1) and (2) display the two frequencies N and 2Ω . Without loss of generality the fixed frame of reference will be chosen so that $n_i = \delta_{i3}$ from now on, with u_3 the vertical velocity component.

The linear inviscid limit for the rotating neutral case, $\Omega \neq 0$, $N = 0$, is firstly recalled as follows. Only equation (1) without the buoyancy force term on the left-hand-side, and equation (3) have to be considered. The linear inviscid limit is obtained by discarding both advection and viscous terms in (1). Without the pressure term, this equation admits sinusoidal solutions for horizontal velocity u_1, u_2 components, with frequency 2Ω . Of course, these pressureless solutions are not valid in the general case, and the pressure term is needed for satisfying the solenoidal constraint (3). The pressure term is responsible for a coupling between horizontal and vertical velocity components, and for the anisotropic dispersion law of internal inertial waves. The last effect is essential since the pressureless linearised equations admit *oscillating* solutions, but not really *propagating waves* solutions. Eliminating velocity in the system of equations (1) and (3) yields

$$\partial_t^2(\nabla^2 p) + 4\Omega^2\nabla_V^2 p = 0 \quad (4)$$

where $\nabla_V^2 = \partial^2/\partial x_3^2$ denotes the vertical part of the Laplacian operator. An illustration of the specific wave properties of inertial waves is given by the experiment of Mc Ewan, whose typical results are shown in the first figure in the Greenspan’s book (1968). Typical cross-shaped structures are visualised when the rotating flow is locally subjected to a harmonic forcing of given frequency σ_0 , with $\sigma_0 < 2\Omega$. In accordance with the normal form of forced solutions $p = e^{-i\sigma_0 t}\mathcal{P}(\mathbf{x})$, the previous pressure equation becomes $\sigma_0^2\nabla_H^2\mathcal{P} + (\sigma_0^2 - 4\Omega^2)\nabla_V^2\mathcal{P} = 0$, showing a change from elliptic to hyperbolic form when σ_0 crosses the

value 2Ω by decreasing values. In addition, the pressure equation exhibits the typical dispersion law

$$\sigma_k = \pm \frac{2\Omega k_3}{k} = \pm 2\Omega \cos \theta_k \quad (5)$$

with $k^2 = k_1^2 + k_2^2 + k_3^2$ for solutions under the form of plane waves $p = P \exp[i(\mathbf{k} \cdot \mathbf{x} - \sigma t)]$. The geometric factor in \mathbf{k} -space, which is exhibited by the dispersion law, is directly related to the conical structure of rays in the experiment, in the forced resonance case $\sigma_k = \sigma_0$, or accordingly $\cos \theta_k = \pm \sigma_0/(2\Omega)$. In the general unforced case where pressure disturbances consist of a dense spectrum of modes with different angles θ_k , different frequencies $|\sigma_k|$ are permitted, ranging from 0 (horizontal wave vectors) to 2Ω (vertical wave vectors). These various frequencies, which are directly related to various orientations for the phases of inertial modes through the angular-dependent dispersion law, underlies a variety of strange behaviours, ranging from linear resonance with a given local forcing (experiment above) to nonlinear third or fourth-order resonances. The celebrated ‘elliptical flow instability’ can be considered as a linear resonance induced by a small additional strain, in which the oblique modes of inertial waves $\cos \theta_k = \pm 1/2$ are selectively amplified in the presence of weak strain.

The paper is organised as follows. Linear approaches, which are useful in both turbulence modelling and stability analyses, are recalled in section 2. They range from ‘homogeneous RDT’ to WKB theories, as the ‘geometrical optics’ used by Lifschitz and Hameiri (1991). Results of the stability analysis of the Stuart vortices in rotating frame are shown and discussed in section 3, with particular emphasis on the three ‘background’ instabilities, namely the centrifugal, elliptic and hyperbolic ones. The problem of *creation* of 2D structure from 3D initially unstructured turbulence in a rotating frame is the core of the paper. The case of nonlinear dynamics, with interactions of inertial waves, in homogeneous rotating turbulence is treated in section 4, and is the most detailed. Additional effects of walls and local forcing are touched upon in section 5, in which results of a numerical study are shown and discussed in connection with the experimental study by Hopfinger *et al.* (1982). The case of stratified turbulence, with and without rotation, is briefly considered in section 6, and nonlinear dynamics is discussed along the same guidelines as pure rotating turbulence is, together with final concluding comments.

2 From RDT to zonal (or local) stability analysis

In the presence of a mean flow, denoted by capital letters (\bar{U}_i, \bar{P}) , equation (1) for the fluctuating components (u_i, p) includes additional ‘advection’ and ‘deformation’ terms in its left-hand-side as follows:

$$\bar{U}_j \partial u_i / \partial x_j + (\partial \bar{U}_i / \partial x_j) u_j. \quad (6)$$

Neglecting nonlinear and viscous terms in equations for (u_i, p) , in the presence of terms (6), is the background for Rapid Distortion Theory (or RDT), introduced by Batchelor and Proudman (1954), not to mention older seminal works by Kelvin, Orr, Prandtl, Taylor ... In neglecting nonlinearity entirely, the effects of interaction of turbulence with itself are supposed small compared with those resulting from mean-flow distortion of turbulence.

Implicit is the idea that the time required for significant distortion by the mean flow is short compared with that for turbulent evolution in the absence of distortion.

For simplified analysis, the case of an *extensional* flow, with space-uniform velocity gradients

$$\bar{U}_i = \lambda_{ij}(t)x_j \quad (7)$$

presents particular interest. If (7) is assumed to be valid in all the space, it is a necessary condition to preserve statistical homogeneity of the fluctuating field. In turn, the gradient of the Reynolds Stress tensor disappears in the equations for the mean, so that there is no feedback of the fluctuating field in the equation governing the mean, and \bar{U}_i has to be a particular solution of Euler equations. Hence, solving the linearized equations which govern (u_i, p) in the presence of a given mean velocity gradient, is exactly the same problem as occurring for the linear stability of the flow (\bar{U}_i, \bar{P}) , with u_i and p small amplitude disturbance to that field.

This ‘RDT’ solution to an initial value problem, is most easily obtained via Fourier synthesis. An elementary Fourier component of the form

$$u_i = a_i(t) \exp[i\mathbf{k}(t) \cdot \mathbf{x}] \quad (8)$$

yields a solution of the problem if \mathbf{k} and a_i satisfy a linear system of simple ordinary differential equations, referred to as Townsend equations. The pressure fluctuation, which is solution of a Poisson equation, is given by an algebraic relationship in term of a_i , whereas time dependency of the wavenumber represents convection of the plane wave $\exp[i\mathbf{k}(t) \cdot \mathbf{x}]$ by the mean flow (7). Likewise, the solution of Townsend equations has the form

$$a_i[\mathbf{k}(t), t] = G_{ij}(\mathbf{k}, t, t_0) a_j[\mathbf{k}(t_0), t_0], \quad (9)$$

where G_{ij} is a spectral Green’s function, which is a real *deterministic* quantity. At this stage, it may be noticed that the RDT for homogeneous turbulence in the presence of mean velocity gradients includes two problems:

- A *deterministic problem*, which consists of solving in the more general way the initial value linear system of equations for a_i . This is done by determining the spectral Green function, which is also the key quantity requested in linear stability analysis.
- A *statistical problem* which is useful for prediction of statistical moments of u_i and p . Interpreting the initial amplitude $a_j(t_0)$ as a random variable with a given dense spectrum, equation (9) yields prediction of statistical moments by products of the basic Green’s function.

Applications to statistics will only be discussed when G_{ij} consists of simple complex exponential, in connection with wavy or steady modes of motion (sections 4 and 6). Exactly the same deterministic problem as the one of ‘homogeneous RDT’ was addressed in the context of flow stability (see, for instance, Bayly 1986, Craik & Criminale 1986), although the two communities seem to be largely unaware of each other’s work. In particular, the stability analysis in terms of time-dependent, distorted, Fourier modes is attributed to Kelvin (1887) by the stability literature. In agreement with the generality of the RDT formulation, which is not restricted to a special case of parallel pure shear

flow (as in Kelvin), I proposed to refer to (8) as ‘Lagrangian Fourier modes’, which are governed by ‘Townsend equations’.

Rotational mean flows yield rather complex RDT solutions, and only the steady case has received much attention. (see Bayly, Holm & Lifschitz, and Craik and coworkers for recent developments in unsteady cases). It can be shown that symmetry of λ^2 and $\lambda_{ii} = 0$ (Craya 1958) imply that λ_{ij} takes the form

$$\lambda = \begin{pmatrix} 0 & S - \Omega_0 & 0 \\ S + \Omega_0 & 0 & 0 \\ 0 & 0 & 0 \end{pmatrix} \quad (10)$$

when axes are chosen appropriately, where $S, \Omega_0 \geq 0$. This corresponds to steady plane flow, combining vorticity $2\Omega_0$ and irrotational straining S . The general RDT problem with arbitrary S and Ω_0 was analysed by Cambon (1982), while experimental realisations of grid turbulence interacting with the mean flow represented by (2.6) were carried out by Leuchter *et al.* (1992). The above class of steady mean flows is also compatible with homogeneity in a frame of reference rotating about an axis perpendicular to the plane of the flow. Cambon *et al.* (1994) give details of RDT calculations for such flows. The limiting case, $S = \Omega_0$ (Townsend 1956), corresponds to simple shearing and forms the borderline between two distinct regimes, namely those in which the mean flow streamlines are closed and elliptic about the stagnation point at the origin ($S < \Omega_0$) and those for which they are open and hyperbolic ($S > \Omega_0$). These two cases will be rediscussed in the next section.

Assuming weak inhomogeneity, turbulence which is fine-scale compared with the overall dimensions of the flow can be treated under RDT by following a notional particle moving with the mean velocity. Particles (fluid elements) are convected by the mean velocity field according to

$$\dot{x}_i = \bar{U}_i(\mathbf{x}, t) \quad (11)$$

Thus, the results obtained for strictly homogeneous turbulence can be extended to the weakly inhomogeneous case, but with a mean velocity gradient matrix $\lambda_{ij}(t)$ which reflects the $\partial \bar{U}_i / \partial x_j$ seen by the moving particle (Hunt 1973). This idea has been formalised in the context of flow stability (see Lifschitz & Hameiri 1991) using an asymptotic approach based on the classical WKB method, which is traditionally used to analyse the ray theoretic limit (i.e. short waves) in wave problems. The solution is written as

$$u_i(\mathbf{x}, t) = a_i(\mathbf{x}, t) \exp[i\Phi(\mathbf{x}, t)/\delta] \quad (12)$$

with a similar expression for the fluctuating pressure, where Φ is a real phase function and δ is a small parameter expressing the small scale of the ‘waves’ represented by (12), while $a_i(\mathbf{x}, t)$ is a complex amplitude which is expanded in power of δ according to the WKB technique. Over distances of $O(\delta)$, one can use a spatial Taylor’s series representation for Φ , up to the linear term, and approximate a_i as constant. It is then apparent that (12) is locally a plane-wave Fourier component of wavenumber

$$k_i(\mathbf{x}, t) = \delta^{-1} \partial \Phi / \partial x_i \quad (13)$$

The amplitude $a_i(\mathbf{x}, t)$ in (12) and the corresponding equation for the fluctuating pressure are expanded as an asymptotic series in powers of δ and the result injected into the

linearised equations without viscosity. At leading order, one finds equations for \mathbf{k} and $a_i^{(0)}$, which have exactly the same form as the Townsend equations (for \mathbf{k} and \mathbf{a} in (8) in homogeneous RDT). These equations are recalled in the next section.

3 Application to local stability of Stuart vortices

The three background instabilities, namely the centrifugal, elliptic and hyperbolic ones, and their alteration by system rotation are not discussed in general here for the sake of brevity (see Kloosterziel & van Heijst, 1991, and Cambon 1999).

The array of Stuart vortices is periodic in the streamwise direction x_1 only, and the vorticity of the eddies has the same sign. The streamfunction is given by

$$\Psi = \ln(\cosh x_2 - \rho \cos x_1) \quad (14)$$

where ρ , $0 < \rho < 1$, characterizes the vorticity distribution inside the vortices. This is a good model of the first instability of the plane mixing layer. The limiting case $\rho = 0$ gives the classic parallel flow with tangent-hyperbolic profile, with no dependency on the streamwise coordinate and no concentrated eddies. The other limit $\rho = 1$ corresponds to an array of concentrated point vortices. In the general case, ρ gives both the ellipticity and the vorticity in the core of the eddies (see fig. 1 for $\rho = 1/3$). The Rossby number is defined as the ratio $Ro = W_0/(2\Omega)$ of core vorticity to system vorticity, with $W_0 = -(1+\rho)/(1-\rho)$. The linear stability approach of Leblanc & Cambon (1998) included both a nonlocal method of normal modes and a particular application of the local analysis, limited to stagnation points. At high values of the spanwise wave number k_3 , both analyses were shown to coincide well with identification of the role of elliptic and hyperbolic points. Especially, the coefficient of amplification of the normal mode was shown to coincide with the one given by the temporal Floquet analysis (see below) around the elliptic stagnation point at the core. Nevertheless, no clear evidence of a centrifugal mode of instability was given by the nonlocal method, likely due to the somewhat low values of ρ investigated, and perhaps due to a lack of numerical resolution. The local method, applied here only to stagnation points, was, of course, not relevant for identifying such a mode. Other numerical results for nonlocal stability in the same case (Stuart vortices in rotating frame) have suggested that a centrifugal mode does exist in the anticyclonic cases (Potylitsin & Peltier 1999). These results, and the relevance of local analysis proved by Sipp *et al.* (1999) for identifying the centrifugal mode in 2D Taylor-Green flow, have suggested to extend the local analysis to streamlines of Stuart vortices other than the stagnation points. This work is in progress (Cambon, Godefert & Leblanc 1999), of which method and typical results are summarized in the following.

Following the WKB analysis of Lifshitz & Hameiri (1991), Townsend equations have to be numerically solved in the rotating frame following different given trajectories ((11) or $\Psi = \text{constant}$ in (14)). The system of linear equations becomes

$$\dot{x}_i = \bar{U}_i \quad (15)$$

$$\dot{k}_i = -\bar{U}_{j,i} k_j \quad (16)$$

$$\dot{a}_i = -[(\delta_{ij} - 2\frac{k_i k_j}{k^2})\bar{U}_{jl} + 2\Omega(\delta_{ij} - \frac{k_i k_j}{k^2})\epsilon_{j3l}]a_l \quad (17)$$

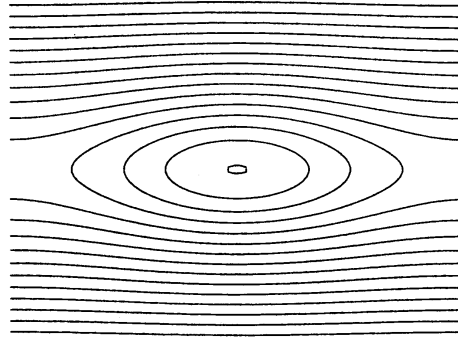


Figure 1: The Stuart flow. Isovalues of the streamfunction (14). Case $\rho = 1/3$.

in the rotating frame. In the above system of ODE, the velocity components \bar{U}_i and the velocity gradient matrix $\bar{U}_{i,j}$ are analytically expressed at any point using (14). These equations are solved given initial data, denoted by capital letters, so that \mathbf{X} is the initial position on the trajectory (Lagrangian coordinate), \mathbf{K} is the Lagrangian wavevector, and \mathbf{A} is the initial amplitude.

Only closed trajectories, identified by the abscissa $0 < x_0 < \pi$, with $\mathbf{X} = (x_0, 0, 0)$ are considered here. The Lagrangian, initial, wave vector is chosen normal to the initial velocity, so that $\mathbf{K} = (\sin \theta_k, 0, \cos \theta_k)$, with $0 \leq \theta_k \leq \pi/2$. The angle $\theta_k = 0$ characterizes *pure spanwise, pressure-less modes*, whereas $\theta_k = \pi/2$ characterises 2D modes. The Green function of the linear system of equations (15-17), as in (9), is numerically computed, after a period T , which corresponds to the time to run a complete loop,

$$a_i(\mathbf{X}, \mathbf{K}, T) = G_{ij}(\mathbf{X}, \mathbf{K}, T, 0)A_j \quad (18)$$

choosing $A_j = \delta_{j1}$, $A_j = \delta_{j2}$, $A_j = \delta_{j3}$, successively. Then the Floquet parameter $\sigma(\mathbf{X}, \mathbf{K}, T)$ related to the modulus s of the maximum eigenvalue of the Floquet matrix G_{ij} in (18) through $\sigma = \ln(s)/T$, is identified for each trajectory, labelled by x_0 , with $\mathbf{X} = (x_0, 0, 0)$, and each initial wavevector, labeled by θ_k .

The distribution of the Floquet parameter is shown for different closed trajectories and different positions of the wave vector in figures 2 and 3. The thick line curve on the bottom plane represents the absolute circulation Γ_a plotted versus x_0 ; this is computed numerically for the different non-circular trajectories. The case $\rho = 1/3$ is considered in figure 2, without rotation, and in figure 3 ($Ro = -2$ at the core). This case was addressed by Leblanc and Cambon (1998). The values of vorticity and ellipticity at the core are $W_0 = -2$ and $E = 1.732$, respectively. These figures enable us to identify the three typical modes and their alteration by system rotation in a clear way, using an inexpensive ‘local’ (trajectory by trajectory) computation. Local analysis is invaluable for substituting the *informative* taxonomy of unstable modes, *hyperbolic*, *elliptic*, *centrifugal*, to the *zoological* one, *braid*, *core*, *edge*, used for instance by Peltier and coworkers since 1994.

As shown in figures 2 and 3, the elliptic mode is captured as an oblique mode whose angular location θ_k and amplification rate σ is found for individual streamlines near the core, in a way consistent with previous RDT and stability analyses for extensional flows (Cambon 1982, Bayly 1986, Cambon *et al.* 1994). In particular, the elliptic mode, which is located at $\theta_k \sim \pi/3$ with no rotation, is shifted towards a spanwise mode $\theta_k \sim 0$ and

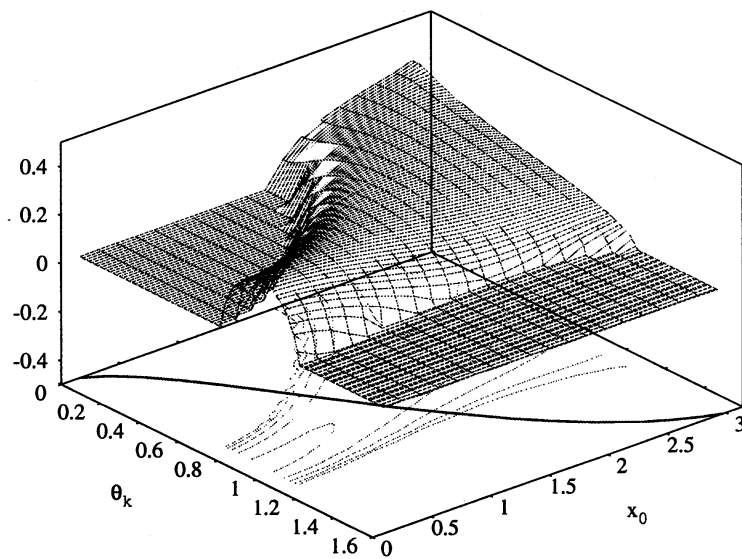


Figure 2: Floquet parameter distribution for different closed trajectories, given by (14) and initialized at $\mathbf{X} = (x_0, 0, 0)$, and for different angles θ_k . The thick curve represents absolute circulation. Case $\rho = 1/3$, $\Omega = 0$. ‘Elliptic’ and ‘hyperbolic’ bumps

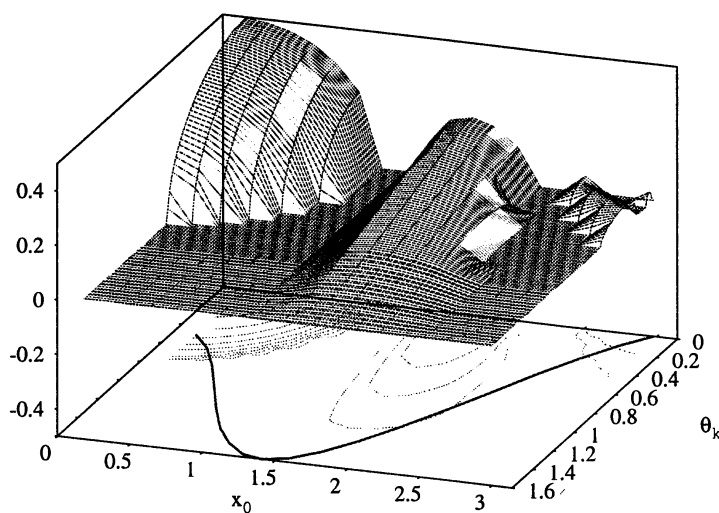


Figure 3: Legend as in fig. 2. Case $\rho = 1/3$, $Ro = -2$. ‘Elliptic’ and ‘Centrifugal’ bumps.

more amplified in the anticyclonic case, in agreement with a maximum amplification for $Ro = -2$. These results are also consistent with the ones of Sipp and coworkers for the flattened Taylor-Green vortices.

The identification of the centrifugal mode in the anticyclonic cases ($Ro < 0$) is also clear and accurate using the local analysis along intermediate streamlines between the core and the periphery. This mode is confirmed to be essentially spanwise ($\theta_k = 0$), and located nearly outward the streamline where absolute circulation reaches a maximum. This characteristic streamline moves towards the periphery when the anticyclonic system rotation is smaller and smaller, so that the centrifugal and the hyperbolic modes can eventually merge. It is confirmed that the unstable hyperbolic mode is essentially spanwise ($\theta_k = 0$), located near peripheral streamlines, and cancelled by large enough rotation rate, without a net distinction between cyclonic and anticyclonic cases.

The most important result is the competition between centrifugal and elliptic instability in the anticyclonic case. For values of the Rossby number around $Ro = -2$, where both types of modes are important, the elliptic instability is shown to be dominant for the lowest value of ρ , as in fig. 3, whereas centrifugal instability is dominant for the cases with weaker core ellipticity. Finally, the centrifugal instability explains the asymmetry of the effect of system rotation and preferential destabilisation of anticyclonic vortices for quasi circular vortices, whereas this explanation is provided by the elliptic instability if the core of the vortex is elliptic enough.

4 Pure rotating homogeneous turbulence

4.1 The transition from 3D to 2D structure: a nonlinear mechanism

In the absence of mean gradients in the rotating frame, the vorticity is governed by

$$\frac{\partial \omega_i}{\partial t} + 2\Omega_j \frac{\partial u_i}{\partial x_j} = \frac{\partial u_i}{\partial x_j} \omega_j - u_j \frac{\partial \omega_i}{\partial x_j} + \nu \frac{\partial^2 \omega_i}{\partial x_j \partial x_j} \quad (19)$$

Only the (linear) second term in the left-hand-side explicitly involves the angular velocity of the rotating frame of reference. Nonlinear and viscous terms are gathered on the right-hand-side. In agreement with the Proudman theorem, a two dimensional state, or $\Omega_j \partial u_i / \partial x_j = 0$, is found in the limit of low Rossby number, high Reynolds number, and slow motions. The first two conditions yield neglecting right-hand-side terms, whereas the last one amounts to neglect the temporal derivative. It is important to point out that the Proudman theorem says only that the *slow manifold* of the linear regime necessarily is the *two-dimensional manifold*, but it cannot predict the transition from 3D to 2D structure, which is a typically nonlinear and unsteady process (see Cambon *et al.*, 1997, for a survey).

For unforced, unbounded, turbulent field, the linear solution consists of superposition of inertial waves (for $u_i, \omega_i, p \dots$), of the form

$$u_i(\mathbf{x}, t) = \int \exp(i\mathbf{k} \cdot \mathbf{x}) [A_i^1 \exp(i\sigma_k t) + A_i^{-1} \exp(-i\sigma_k t)] d^3 \mathbf{k} \quad (20)$$

where the $A_i^\epsilon(\mathbf{k})$, $\epsilon = \pm 1$, are projections of the initial disturbance field onto the two eigenmodes of linearised equations. Of course, Fourier synthesis is used for convenience, or $u_i(\mathbf{x}, t) = \int \exp(i\mathbf{k} \cdot \mathbf{x}) \hat{u}_i(\mathbf{k}, t) d^3\mathbf{k}$, so that we do not discuss a possible replacement of the integral operator in (20) by a discrete summation. Anyway, the dispersion law for transverse pressure waves (5) is recovered as $\sigma_k = \pm 2\Omega \frac{k_3}{k}$ and the slow manifold is recovered as the wave plane orthogonal to the rotation axis, for $k_3 = 0$ which corresponds to $\partial/\partial x_3 = 0$ in physical space. According to (20), the linear solution only describes phase-turbulence, and conserves the spectral density of energy, or $\hat{u}_i^* \hat{u}_i$, so that the transition from 3D to 2D turbulence must be interpreted as an angular drain of energy from oblique wavevectors $k_3/k \neq 0$ towards the waveplane $k_3 = 0$, energy drain which is mediated by nonlinear interactions.

4.2 wave turbulence and closure theories

Equation (1) with zero buoyancy and with incompressibility constraint (3) becomes

$$(\partial_t + \nu k^2 + i\epsilon\sigma_k)\xi_\epsilon(\mathbf{k}, t) = \sum_{\epsilon', \epsilon'' = \pm 1} \int_{\mathbf{p}+\mathbf{q}=\mathbf{k}} m_{\epsilon\epsilon'\epsilon''} \xi_{\epsilon'}(\mathbf{p}, t) \xi_{\epsilon''}(\mathbf{q}, t) d^3\mathbf{p} \quad (21)$$

with $\epsilon = \pm 1$, after projection onto the normal modes of \mathbf{u} in Fourier space. The basis of eigenmodes (see [10], [31], [13]) is used to express the Fourier coefficient $\hat{\mathbf{u}}$ as

$$\hat{\mathbf{u}} = \xi_+ \mathbf{N}(\mathbf{k}) + \xi_- \mathbf{N}(-\mathbf{k}) = \sum_{\epsilon = \pm 1} \xi_\epsilon \mathbf{N}(\epsilon\mathbf{k}), \quad (22)$$

with

$$\xi_\epsilon = \hat{\mathbf{u}} \cdot \mathbf{N}(-\epsilon\mathbf{k}), \quad \epsilon = \pm 1, \quad (23)$$

Equation (21) yields exact separation between the linear, diagonal, operator in the left-hand-side, and the triadic nonlinear operator in the right-hand-side. Using (21), the ‘rapid distortion’, or equivalently the ‘linear inviscid’ limit, as in (20), is simply

$$\xi_\epsilon(\mathbf{k}, t) = \exp[i\epsilon\sigma_k(t)] \xi_\epsilon(\mathbf{k}, 0) \quad (24)$$

instead of $\hat{u}_i(\mathbf{k}, t) = G_{ij}(\mathbf{k}, t, t_0) \hat{u}_j(\mathbf{k}, t_0)$ (general RDT solution, without advection, see (9)). Replacing the initial data at fixed $t_0 = 0$ in (24) by a new unknown variable, say a_ϵ , so that

$$\xi_\epsilon(\mathbf{k}, t) = \exp[i\epsilon\sigma_k t] a_\epsilon(\mathbf{k}, t) \quad (25)$$

an equation for a_ϵ is readily derived from (21). Using the above transformation (24) (which amounts to the ‘Poincaré transformation’ used by [1] in the case of pure rotation), the nonlinear dynamics of a_ϵ is easily shown to be

$$\begin{aligned} \dot{a}_\epsilon = & \sum_{\epsilon', \epsilon'' = \pm 1} \int_{\mathbf{k}+\mathbf{p}+\mathbf{q}=\mathbf{0}} \exp[2i\Omega(\epsilon \frac{k_{\parallel}}{k} + \epsilon' \frac{p_{\parallel}}{p} + \epsilon'' \frac{q_{\parallel}}{q})t] \times \\ & \times m_{\epsilon\epsilon'\epsilon''}(\mathbf{k}, \mathbf{p}) a_{\epsilon'}^*(\mathbf{p}, t) a_{\epsilon''}^*(\mathbf{q}, t) d^3\mathbf{p} \end{aligned} \quad (26)$$

which is driven by the phase term

$$\exp[i(\epsilon\sigma_k + \epsilon'\sigma_p + \epsilon''\sigma_q)(t - t')] \quad (27)$$

Indeed, the zero value of the phase of the above complex exponential characterises the resonant condition, and the simultaneous conditions

$$\epsilon\sigma_k + \epsilon'\sigma_p + \epsilon''\sigma_q = 0 \text{ with } \mathbf{k} + \mathbf{p} + \mathbf{q} = \mathbf{0}$$

gives the resonant surfaces. At small Rossby number, the long-time behaviour is dominated by near-resonant interactions, and a qualitative analysis of Waleffe (1993) has shown how resonant interactions can concentrate energy towards the 2D manifold. More generally, it is possible to directly construct equations for ‘slow’ amplitude square and cross-correlations, or $\langle a_+^* a_+ \rangle$, $\langle a_-^* a_- \rangle$, $\langle a_+^* a_- \rangle$, from the above equations (26). These quantities are kept constant in the ‘RDT’ limit, whereas the nonlinear terms responsible for their slow evolution are constructed, using either asymptotic developments of weak wave-turbulence or suitably generalized two-point closures. In order to connect that with classic turbulence theory, we will proceed in a slightly different way, by considering a fully anisotropic second order spectral tensor and related transfer tensor. The second-order spectral tensor $\Phi_{ij}(\mathbf{k}, t)$, is the Fourier transform of the two-point covariance matrix

$$\langle u_i(\mathbf{x}, t) u_j(\mathbf{x}', t) \rangle \quad (28)$$

and its more general expression for homogeneous anisotropic turbulence is

$$\Phi_{ij} = \begin{pmatrix} 0 & 0 & 0 \\ 0 & e + Z_r & Z_i - i\mathcal{H}/k \\ 0 & Z_i + i\mathcal{H}/k & e - Z_r \end{pmatrix} \quad (29)$$

using an orthonormal frame of reference, associated with polar-spherical coordinates (k, θ, ϕ) of \mathbf{k} in Fourier space, in close connection with the Craya-Herring decomposition for the velocity field. Hence Φ_{ij} can be expressed as a sum of different contributions, in term of the scalars e (energy spectrum), Z (polarisation anisotropy), with $Z = Z_r + iZ_i$ complex, and \mathcal{H} (helicity spectrum), which all depend on \mathbf{k} . Isotropic turbulence is characterized by $e(k, \theta, \phi, t) = E(k, t)/(4\pi k^2)$, $Z = \mathcal{H} = 0$, so that the real part of Φ_{ij} , which is involved in classic one-point correlations, involve e and Z contributions as follows

$$Re(\Phi_{ij}) = \underbrace{\frac{E(k)}{4\pi k^2} P_{ij}}_{\text{Pure isotropic part}} + \underbrace{\left(e(k, \theta, \phi) - \frac{E(k)}{4\pi k^2} \right) P_{ij}}_{\text{Directional anisotropy}} + \underbrace{Re(Z N_i N_j)}_{\text{Polarisation anisotropy}} \quad (30)$$

(see [13] for details, Re denotes the real part of a complex quantity, P_{ij} is the classical projection operator, and N_i is the eigenvector as in (22)). It is clear from the above equation that the anisotropy is twofold. A lessening of dimensionality is only reflected by a nonzero value of the second term. Indeed, the directional anisotropy, which is expressed by a departure of e from a spherical equidistribution, is extreme in a pure two-dimensional state, where e is concentrated onto the plane $k_3 = 0$. The set e, Z, \mathcal{H} is governed by the following system of equations

$$\left(\frac{\partial}{\partial t} + 2\nu k^2 \right) e = T^e \quad (31)$$

$$\left(\frac{\partial}{\partial t} + 2\nu k^2 + 4i \cos \theta_k \right) Z = T^Z \quad (32)$$

$$\left(\frac{\partial}{\partial t} + 2\nu k^2\right)h = T^h \quad (33)$$

in which the right-hand-sides reflect nonlinear transfer terms. Of course, the set (e, Z, \mathcal{H}) is immediately derived from the set of amplitude correlations $\langle a_+^* a_+ \rangle$, $\langle a_-^* a_- \rangle$, $\langle a_+^* a_- \rangle e^{-4i \cos \theta_k t}$ through linear combination, and the generalized transfer terms T^0 are cubic in terms of these amplitudes.

In the general derivation of EDQN (Eddy Damped Quasi Normal) closures, detailed anisotropy is preserved, and the structure of linear propagators is an essential ingredient. The complete equation (see Cambon & Scott 1999) is not recalled for the sake of brevity. A complete closure of generalized transfer terms (T^e, T^z, T^h) in term of (e, Z, \mathcal{H}) is eventually derived using the decomposition (30) and the following Kraichnan's 'response tensor'

$$G_{ij}^{QN} = Re[N_i N_j^* \exp(i\sigma_k(t-t'))] \exp[-\mu_k(t-t')] \quad (34)$$

in which the viscous + eddy damping term μ_k has to be specified, or is governed by additional dynamical equations in more complex DIA or TFM versions. In the case of strong rotation, its role is only to ensure suitable convergence of temporal integrals, and its shape is unimportant. The final step in applying the procedure is the so-called 'markovianization'. In our context, this amounts to separate in the integrands terms considered as rapidly evolving, and terms, linked to a_ϵ in (25), considered as slowly evolving. Only in the latter, the non-instantaneous dependency with respect to the past time t' is reduced to an instantaneous dependency, making $t' = t$. The first non-trivial application of this procedure to turbulence with waves was called EDQNM2. His advantage was to exhibit a generic closure relationship, for instance

$$T^e = \sum_{\epsilon, \epsilon', \epsilon'' = \pm 1} \int_{k+p+q=0} \frac{S^{QN}(\epsilon \mathbf{k}, \epsilon' \mathbf{p}, \epsilon'' \mathbf{q})}{\mu_k + \mu_p + \mu_q + 2i\Omega(\epsilon \cos \theta_k + \epsilon' \cos \theta_p + \epsilon'' \cos \theta_q)} d^3 \mathbf{p} \quad (35)$$

in which the same phase term as in (27) naturally appears through the three-fold product of Green's functions (34). The main result of EDQNM2, when contrasted with a high resolution $(128 \times 128 \times 512)$ Large-Eddy-Simulation, is shown on fig. 4. This is the trend to concentrate the spectral density of energy $e(k, \cos \theta_k, t)$ towards the wave plane normal to the rotation axis, or $\cos \theta_k = 0$, in agreement with a partial two-dimensionnalisation mediated by the nonlinear spectral transfer T^e in (31).

Recently, it was shown that the treatment of the 'rapid' phase in the oscillating term Z in (32) was not consistent with a systematic separation rapid-slow based upon (25) and its statistical moments up to the third order, and an improved version, EDQNM3, was constructed. Even if the two versions yield similar numerical results in rotating turbulence started with almost isotropic initial data, realizability is not ensured by EDQNM2 for any initial data, and localized lack of realizability were exhibited in the stably stratified case (van Haren 1993). As a bonus, a realisable, simplified asymptotic model AQNM is being derived from the EDQNM3 version (Scott 1999) in the limit $\mu_k \ll \Omega$. This model gives the opportunity to investigate the limit of very small Rossby numbers, very high Reynolds, and very long time, limit which cannot be captured by standard pseudo-spectral DNS, and even by standard numerical calculations of discretized EDQNM2-3 versions.

Going back to experimental (Jacquin *et al.*, 1990) and numerical (more or less classic DNS-LES) experiments, which only deal with short times and moderate Reynolds

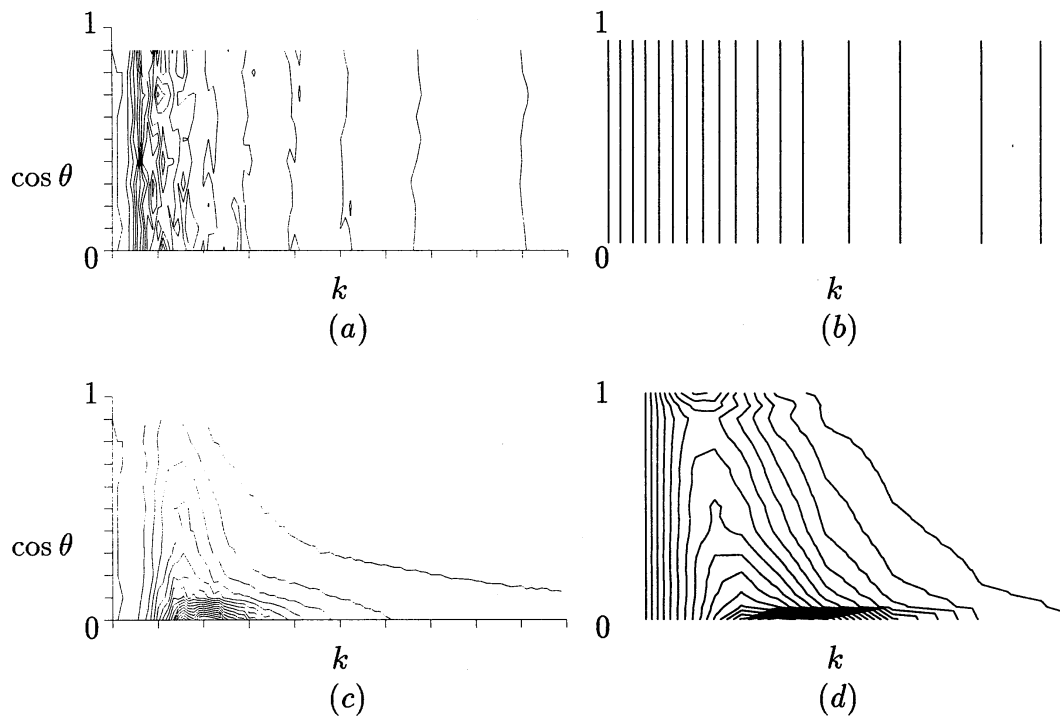


Figure 4: Isolines of kinetic energy for LES computations (a) at $\Omega = 0$ at time $t/\tau = 427$, (b) EDQNM2 with $\Omega = 0$; (c) LES with $\Omega = 1$ at $t/\tau = 575$; and (d) EDQNM2 calculation with $\Omega = 1$ at time $t/\tau = 148$. The vertical axis bears $\cos \theta_k$ (from 0 to 1 upwards) and the horizontal one the wave number k . (Courtesy from Cambon *et al.* 1997)

numbers, they confirm that the nonlinear tendency to create columnar structures is very subtle and cannot yield to well organised arrays of 2D vortices. The eventual appearance of such ‘rotors’ in other low resolution DNS or LES in periodic boxes is only a numerical artefact. In an actual experiment or —explicitly inhomogeneous— numerical simulation, however, the nonhomogeneous forcing and/or the presence of solid boundaries can enforce the creation of such organised vortices.

5 Additional role of forcing and solid walls

Although they confirm the significant anisotropisation linked to partial two-dimensionalisation, physical experiments and high resolution DNS and LES do not really show creation of coherent quasi-2D vortices, as far as the conditions for reproducing homogeneity are fulfilled. One of this condition is to stop the computation when the most amplified integral lengthscale becomes of the same order of magnitude as the length of the computational box. A good compromise to reach higher elapsed times without developing spurious anisotropy was obtained by Mansour with an elongated computational box with length in axial direction four times the length in other two directions (corresponding to $512 \times 128 \times 128$ LES used in Cambon *et al.* 1997). Apparently more complete two-dimensionalisation with creation of strong axial rotors was shown in the low resolution 64^3 LES of Bartello *et al.* (1994), but this is a numerical artifact due to blocking the integral lengthscales when the computation is performed for too large elapsed times.

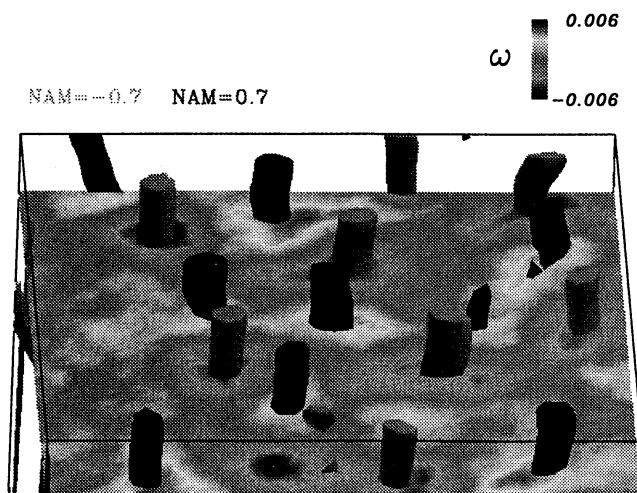


Figure 5: Vortex structures identified by NAM iso-values (tubes) and vorticity iso-values. (Courtesy from Godefert & Lollini 1999)

Another difference of the latter study with DNS and LES studies, in which homogeneity is fulfilled (Bardina et al. 1985, Cambon et al. 1997), was the rise of a two-component limit for the Reynolds stress tensor in [3] ($\overline{u_3^2} \ll \overline{u_1^2} \sim \overline{u_2^2}$), in close connection with interference with periodic boundaries. The last numerical study has suggested that boundary effects are important for reinforcing the rise of coherent axial vortices. Hence a numerical simulation of rotating turbulence between two solid parallel walls has been performed by Godefert & Lollini (1999) by means of a pseudo-spectral code. Another, more important, motivation for the DNS was to try to reproduce the essential results of the experiment by Hopfinger *et al.* (1982) in which confinement and local forcing are additional, essentially inhomogeneous, effects with respect to the Coriolis force. Typical DNS results are briefly presented and discussed as follows. A transition is shown to occur between the region close to the forcing and an outer region in which coherent vortices appear, the number of which depends on the Reynolds and Rossby numbers. Identification of vortices is shown in fig. 5 using both iso-vorticities (noisy spots) and a specific criterion (Normalized Angular Momentum), which was suggested by experimentalists in PIV for obtaining smooth isovalues. Asymmetry in terms of cyclones-anticyclones is mainly induced by the Ekman pumping near the solid boundaries, yielding helical trajectories. This is illustrated in fig. 6, in which a pair cyclone-anticyclone is isolated. Even if the Ekman pumping generates a three-component motion, the presence of the horizontal walls, and the presence of the forcing in a horizontal plane between them, are essential for enforcing coherent vortices.

Nevertheless, and in contrast with the experimental results, the asymmetry cyclones-anticyclones was not obtained in term of number and intensity, but for a case. In the same way, the typical distance between adjacent vortices is of the same order of magnitude as their diameter, and the Rossby number in their core is close to one. It was expected

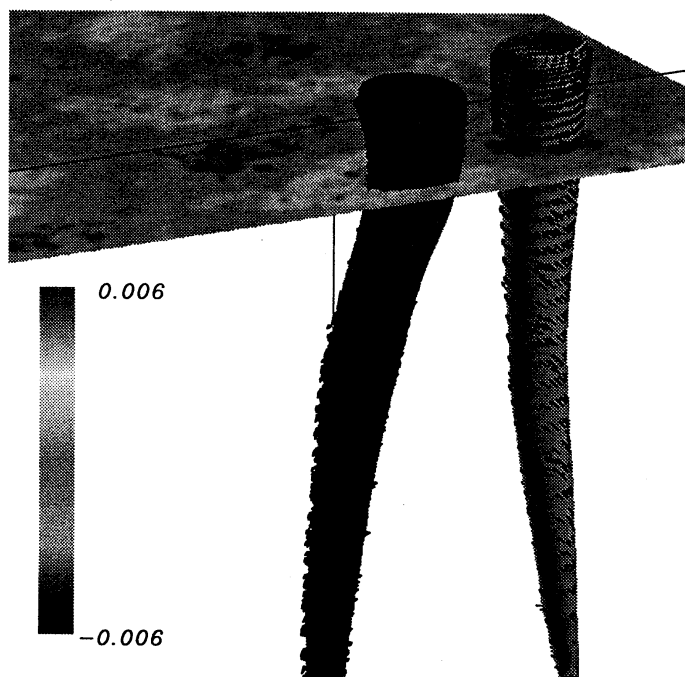


Figure 6: Selected pair of cyclonic-anticyclonic eddy structures. (Courtesy from Godeferd & Lollini 1999)

that for a given symmetric distribution of more intense and concentrated vortices (higher Rossby number), the centrifugal and elliptic instabilities could act in destabilizing the anticyclones, so that dominant cyclones could emerge, as in the physical experiment. It seems that the insufficiently high Reynolds number is responsible for the lack of intensity and concentration. Hence, the conditions of stability —rediscussed in conclusion— are no relevant for strongly favouring the cyclonic eddies, but they could do that for higher Reynolds DNS or LES.

6 Concluding comments

6.1 Stably-stratified homogeneous turbulence with and without rotation

In this case, which is not discussed in detail for the sake of brevity, it is necessary to reintroduce the buoyancy force term b in eq. (1). Using a special frame of reference and a unique vector for u_i and b , the initial five components-problem (u_1, u_2, u_3, p, b) reduces to a three-component one, with three eigenmode amplitudes $(\xi_0, \xi_{+1}, \xi_{-1})$. Two of them characterise wavy motion ($\epsilon = \pm 1$), similarly to the case of pure rotation, but the presence of a steady mode ($\epsilon = 0$) is an important new thing. The steady mode corresponds to the solenoidal part of the horizontal velocity field, or ‘vortex’ mode (Riley et al. 1982) in pure stratified flows, and to the ‘quasi-geostrophic’ mode in the combined rotating-stratified flow. Hence, the case of stably stratified turbulence is very different from the case of pure rotation, even if the gravity waves present strong analogies with inertial waves, and if all

the equations of section 5 can have a similar form (but with $\epsilon = \pm 1$ and $\epsilon = 0$ in (21) and (26)).

The vortex mode is present for any wavevector orientation, and contains half the total kinetic energy in isotropic turbulence. Pure vortex interactions were found to be dominant; resonant conditions are obtained with $\epsilon = \epsilon' = \epsilon'' = 0$ in (21) and (26) with no need to restrict to resonant surfaces as for resonant wave interactions. Godefert and Cambon (1994) have shown that the spectral energy concentrates towards vertical wavenumbers $k_{\perp} \sim 0$. These wavenumbers correspond to horizontally (because \mathbf{k} and $\hat{\mathbf{u}}$ are perpendicular) stratified turbulent structures with dominantly horizontal, low-frequency motions. As for the ‘2D transition’ expected in pure rotation, a new dynamical insight was given to the collapse of vertical motion and layering expected in stably stratified turbulence. Only recently, reintroducing a small but significant vortex part in their wave turbulence analysis, Caillol and Zeitlin (1999) found that: *‘The vortex part obeys a limiting slow dynamics equation exhibiting vertical collapse and layering which may contaminate the wave-part spectra’*. This is in complete agreement with the main finding of [18]. It is important to point out that this result reflects a scrambling of any triadic interactions, like $(0 \pm 1 \pm 1)$, including at least one wave mode, so that the pure vortex interaction (000) becomes dominant. The corresponding ‘vortex energy transfer’ is strongly anisotropic, it does not yield a classic cascade (which would contribute to dissipate the energy) but instead yields the angular drain of energy which condensates the energy towards vertical wave-vectors, in agreement with vertical collapse and layering. At much larger times, the transfer terms including wave contribution could become significant through resonant wave triads, but this would occur in a velocity field yet strongly altered (thence strongly anisotropic) by collapse and layering. As for the case of pure rotating turbulence, linear ‘RDT’ solutions as (20), even with an additional steady term A_i^0 , are not capable of predicting irreversible collapse and layering of the velocity field. Nevertheless, they can present interest for calculating two-time second order Eulerian correlations, in connection with prediction of a plateau for lagrangian one-particle vertical dispersion (Kaneda & Ishida, Nicolleau & Vassilicos, papers to appear).

The case of combined effects of rotation and stratification presents particular interest in the geophysical context for large enough horizontal length scales, and is the subject of many works in progress, using weakly nonlinear wave-turbulence theories and accurate DNS data. ([1], Kimura & Herring)

6.2 General comments

- Anisotropic ‘two-point closures’ ([13], [14]) versus ‘wave-turbulence’ theories ([1], [7], [32]).

As for ‘RDT’ and ‘linear stability’ communities, there is too few common works on possible points of contact between the two communities. An important common formalism exists, provided the closures be using the bases of eigenmodes without isotropy assumption. The presence of a damping term in the closures, as μ_k in (34) plays a particular role, even if very small, to regularise the ‘resonance operator’, which often reduces to a Dirac Delta function in wave-turbulence theories.

- Anisotropy versus structure.

Anisotropic spectral description, with angular dependence of spectra and cospectra in Fourier space, allows to quantify columnar or pancake structuring in physical space. Among various indicators of the thickness and width of pancakes, which can be readily derived from anisotropic spectra, integral lengthscales related to different components and orientations are the most useful.

- Homogeneous versus confined turbulence.

Vertical confinement and local forcing were shown to favour the emergence of organised eddies, in the rotating flow, even if the Ekman layer and the forcing generated more three-dimensionality at small scale. More generally, interaction of geometry with the ‘natural’ development of columnar/pancake structures has to be studied in the general case.

- Structure versus stability analysis.

This topic could link the two parts of our survey of rotating flows: stability analysis of preexisting coherent vortices, and creation of structures through nonlinearity, confinement and forcing. But the vortices appearing in fig. 5 seem to be too weak to be affected by the centrifugal and/or elliptic instabilities discussed in section 3, so that a clear asymmetry in term of cyclonic and anticyclonic eddies was not found. For the stably stratified case, a recent ‘zig-zag’ instability (Billant & Chomaz 1999) was recently proposed to explain the layering (see also Dritschel *et al.*, 1999, in the different context of quasi-geostrophic flows with both stable stratification and system rotation). The typical thickness of the slices, however, is likely much larger than the one seen in a typical turbulent stratified flow. Even if linear stability of preexisting large coherent structures can give qualitative information about the geometry of columnar/pancake fine structures, nonlinear (and nonisotropic) cascade and dissipation remains essential features to predict typical length scales.

References

- [1] BABIN, A., MAHALOV, A. & NICOLAENKO, B. 1998. *Theor. Comput. Fluid Dynamics* **11**, 215–235.
- [2] BARDINA, J., FERZIGER, J. M., ROGALLO, R. S. 1985. ‘Effect of rotation on isotropic turbulence: computation and modelling’, *J. Fluid Mech.* **154**, 321–326.
- [3] BARTELLO, P., MÉTAIS, O., LESIEUR, M. 1994. ‘Coherent structure in rotating three-dimensional turbulence’, *J. Fluid Mech.* **273**, 1–29.
- [4] BATCHELOR, G. K. 1953. ‘The theory of homogeneous turbulence’, Cambridge University, Cambridge.
- [5] BATCHELOR, G. K., PROUDMAN I. 1954 ‘The effect of rapid distortion in a fluid in turbulent motion’, *Q. J. Mech. Appl. Maths*, 7–83.
- [6] BAYLY, B. J. 1986 ‘Three-dimensional instability of elliptical flow’, *Phys. Rev. Lett.*, 57–2160.

- [7] BENNEY, D. J., SAFFMAN, P. G. 1966. 'Nonlinear interactions of random waves in a dispersive medium' *Proc. R. Soc. London, Ser. A* **289**, 301–320.
- [8] BILLANT, P., CHOMAZ, J. M. 1999 'Experimental evidence for a zigzag instability of a vertical columnar vortex pair in a strongly stratified fluid' *J. Fluid Mech.*, submitted (see also *Euromech* 396)
- [9] CAILLOL, P. AND ZEITLIN, W. 1999. 'Kinetic equations and stationary energy spectra of weakly nonlinear internal gravity waves' *Dyn. Atm. Oceans*, to appear.
- [10] CAMBON, C. 1982. 'Etude spectrale d'un champ turbulent incompressible soumis à des effets couplés de déformation et de rotation imposés extérieurement', *Thèse de Doctorat d'État*, Université de Lyon, France.
- [11] CAMBON, C. 1999. 'Stability of vortex structures in a rotating frame' *Proc. S.T.S.V.D., INI turbulence programme, Cambridge*
- [12] CAMBON C., BENOIT J.P., SHAO L., JACQUIN L. 1994 'Stability analysis and large eddy simulation of rotating turbulence with organized eddies', *J. Fluid Mech.* **278**, 175–200.
- [13] CAMBON, C., MANSOUR, N. N. & GODEFERD, F. S. 1997. 'Energy transfer in rotating turbulence' *J. Fluid Mech.* **337**, 303–332
- [14] CAMBON, C. & SCOTT, J. F. 1999. 'Linear and nonlinear models of anisotropic turbulence' *Ann. Rev. Fluid Mech.* **31**, 1–53
- [15] CRAIK, A. D. D., CRIMINALE, W. O. 1986. 'Evolution of wavelike disturbances in shear flows: a class of exact solutions of the Navier-Stokes equations', *Proc. R. Soc. Lond. A* **406**, 13–26.
- [16] CRAYA A. 1958. 'Contribution à l'analyse de la turbulence associée à des vitesses moyennes', *P.S.T. n° 345*. Ministère de l'air. France.
- [17] DRITSHEL, D., G., TORRE JUÁREZ, M., AMBAUM, M. H. P. 1999 'The three-dimensional vortical nature of atmospheric and oceanic turbulent flows' *Phys. Fluids*, to appear.
- [18] GODEFERD, F. S. & CAMBON, C. 1994. 'Detailed investigation of energy transfers in homogeneous stratified turbulence' *Phys. Fluid* **6**, 2084–2100.
- [19] GODEFERD, F. S., LOLLINI, L. 1999. 'Direct numerical simulations of turbulence with confinement and rotation', *J. Fluid Mech.* **393**, 257–307.
- [20] GREENSPAN, H. P. 1968. 'The theory of rotating fluids', Cambridge University Press.
- [21] HOPFINGER, E. J., BROWAND, F., K., GAGNE, Y. 1982. 'Turbulence and waves in a rotating tank', *J. Fluid Mech.* **125**, 505.
- [22] HUNT, J. C. R. 1973. 'A theory of turbulent flow around two-dimensional bluff bodies', *J. Fluid Mech.* **61**, 625–706.

- [23] JACQUIN L., LEUCHTER O., CAMBON C., MATHIEU J. 1990. 'Homogeneous turbulence in the presence of rotation', *J. Fluid Mech.* **220**, 1–52.
- [24] KLOOSTERZIEL, R. C., VAN HEIJST, G. J. F. 1991. 'An experimental study of unstable barotropic vortices in a rotating fluid', *J. Fluid Mech.* **223**, 1–24.
- [25] LEBLANC S., CAMBON C. 1998. 'The effect of the Coriolis force on the stability of the Stuart vortices', *J. Fluid Mech.* **357**, 353–379
- [26] LEUCHTER O., BENOIT J. P., CAMBON C. 1992. 'Homogeneous turbulence subjected to rotation-dominated plane distortion', *Fourth Turbulent Shear Flows*. Delft University of Technology.
- [27] LIFSCHITZ A., HAMEIRI E. 1991. 'Local stability conditions in fluid dynamics', *Phys. Fluids A* **3**, 2644–2641.
- [28] POTYLITSIN, P. G. & PELTIER, W. R. 1999. 'Three-dimensional destabilisation of Stuart vortices: the influence of rotation and ellipticity', *J. Fluid Mech.*, to appear.
- [29] RILEY, J. J., METCALFE, R. W., WEISMAN, M. A. 1981 'DNS of homogeneous turbulence in density stratified fluids' *Proc. AIP conf. on nonlinear properties of internal waves*, edited by B. J. West, AIP, New York, 79–112.
- [30] SIPP, D., LAUGA, E., JACQUIN, L. 1999. 'Vortices in rotating systems: centrifugal, elliptic and hyperbolic type instabilities', *Phys. Fluids*, to appear.
- [31] WALEFFE, F. 1993 'Inertial transfers in the helical decomposition' *Phys. Fluid A*, **5**, 677–685.
- [32] ZAKHAROV, V. E., L'VOV, V. S., FALKOWICH, G. 1992. *Kolmogorov spectra of turbulence. I. Wave turbulence*. Springer series in nonlinear dynamics. Springer Verlag